

RESEARCH

Open Access



# *LncRNA-TBP* mediates TATA-binding protein recruitment to regulate myogenesis and induce slow-twitch myofibers

Manting Ma<sup>1,2</sup>, Bolin Cai<sup>1,2</sup>, Zhen Zhou<sup>1,2</sup>, Shaofen Kong<sup>1,2</sup>, Jing Zhang<sup>1,2</sup>, Haiping Xu<sup>1,2\*</sup>, Xiquan Zhang<sup>1,2</sup> and Qinghua Nie<sup>1,2\*</sup>

## Abstract

**Background** Skeletal muscle is comprised of heterogeneous myofibers that differ in their physiological and metabolic parameters. Of these, slow-twitch (type I; oxidative) myofibers have more myoglobin, more mitochondria, and higher activity of oxidative metabolic enzymes compared to fast-twitch (type II; glycolytic) myofibers.

**Methods** In our previous study, we found a novel *LncRNA-TBP* (for “LncRNA directly binds TBP transcription factor”) is specifically enriched in the soleus (which has a higher proportion of slow myofibers). The primary myoblast cells and animal model were used to assess the biological function of the *LncRNA-TBP* in vitro or in vivo. Meanwhile, we performed a RNA immunoprecipitation (RIP) and pull-down analysis to validate this interaction between *LncRNA-TBP* and TBP.

**Results** Functional studies demonstrated that *LncRNA-TBP* inhibits myoblast proliferation but promotes myogenic differentiation in vitro. In vivo, *LncRNA-TBP* reduces fat deposition, activating slow-twitch muscle phenotype and inducing muscle hypertrophy. Mechanistically, *LncRNA-TBP* acts as a regulatory RNA that directly interacts with TBP protein to regulate the transcriptional activity of TBP-target genes (such as *KLF4*, *GPI*, *TNNI2*, and *CDKN1A*).

**Conclusion** Our findings present a novel model about the regulation of *LncRNA-TBP*, which can regulate the transcriptional activity of TBP-target genes by recruiting TBP protein, thus modulating myogenesis progression and inducing slow-twitch fibers.

**Keywords** *LncRNA-TBP*, RNA binding proteins (RBPs), TBP, Myogenesis, Muscle phenotype transformation

## Background

Skeletal muscles constitute approximately 35% of the body weight and main resources of animal protein for human consumption. Abnormal regulation of skeletal muscle-specific genes leads to various muscle diseases that development directly influences animal meat quantity and quality [1–3]. Myogenesis is a highly ordered process during which muscle stem cell proliferation, migration, differentiation, and fusion are activated to form myofibers [4].

Skeletal muscle is composed of different types of myofibers, which are mainly differentiated by the

\*Correspondence:

Haiping Xu  
music-three@163.com  
Qinghua Nie  
nqinghua@scau.edu.cn

<sup>1</sup> Lingnan Guangdong Laboratory of Modern Agriculture & State Key Laboratory for Conservation and Utilization of Subtropical Agro-Bioresources, College of Animal Science, South China Agricultural University, Guangzhou 510642, Guangdong, China

<sup>2</sup> Guangdong Provincial Key Lab of Agro-Animal Genomics and Molecular Breeding, and Key Laboratory of Chicken Genetics, Breeding and Reproduction, Ministry of Agriculture, Guangzhou 510642, Guangdong, China



© The Author(s) 2023. **Open Access** This article is licensed under a Creative Commons Attribution 4.0 International License, which permits use, sharing, adaptation, distribution and reproduction in any medium or format, as long as you give appropriate credit to the original author(s) and the source, provide a link to the Creative Commons licence, and indicate if changes were made. The images or other third party material in this article are included in the article's Creative Commons licence, unless indicated otherwise in a credit line to the material. If material is not included in the article's Creative Commons licence and your intended use is not permitted by statutory regulation or exceeds the permitted use, you will need to obtain permission directly from the copyright holder. To view a copy of this licence, visit <http://creativecommons.org/licenses/by/4.0/>. The Creative Commons Public Domain Dedication waiver (<http://creativecommons.org/publicdomain/zero/1.0/>) applies to the data made available in this article, unless otherwise stated in a credit line to the data.

expression of heavy chain myosin and the reliance on oxidative phosphorylation [5]. Compared to fast-twitch (type II; glycolytic) myofibers, slow-twitch (type I; oxidative) myofibers have more myoglobin, more mitochondria, and higher activity of oxidative metabolic enzymes [6, 7]. Under certain conditions, fast-twitch myofibers and slow-twitch myofibers can transform into each other [8].

Transcriptional activation is a major step in the regulation of gene expression during development. TATA-binding protein (TBP) and 12–15 associated factors (TAFs) together form the pre-initiation complex (PIC), which as an obligate step leading to transcription [9, 10]. In mice, a large polyQ repeat in TBP causes primary muscle degeneration and decreases the association of MyoD with TBP and DNA promoters [11]. Recent studies have demonstrated that the TBP associated factor (TAF9b) plays an important role in neurodevelopmental and mental disorders. As a coactivator that stabilized the structure of P53, it also participates in P53-mediated apoptosis and cell cycle regulation [12–15].

Long noncoding RNAs (lncRNAs), a novel class of regulatory RNAs, are commonly defined as transcribed RNAs with sizes ranging from 200 bp to >100 kb and not translated to protein [16]. Substantial evidences have shown that lncRNAs play critical regulatory roles in diverse biological processes and diseases, such as skeletal muscle development and muscle disorders [17, 18]. Based on our previous RNA-sequencing (RNA-seq) analysis, we screened and identified an lncRNA (MSTRG.6038.1), which differentially expressed between pectoralis major (PEM, which is mainly composed of fast-twitch fibers) and soleus (SOL, which has a higher proportion of slow muscle fibers) in 7-week-old Xinghua chicken, was named “*LncRNA-TBP*” (for “LncRNA directly binds TBP transcription factor”). Functional studies demonstrated that *LncRNA-TBP* inhibits myoblast proliferation but promotes myogenic differentiation as well as reduces fat deposition, activating slow-twitch muscle phenotype and reducing muscle atrophy. Mechanistically, *LncRNA-TBP* acts as a regulatory RNA that directly interacts with TBP protein to regulate the transcriptional activity of TBP-target genes (such as *KLF4*, *GPI*, *TNNI2*, and *CDKN1A*).

## Materials and methods

### Ethics statement

The experimental animals were chickens of Chinese local breeds. All animal studies were sanctioned by the Institutional Animal Care and Use Committee at the South China Agricultural University. All the experiments were performed according to the regulations and guidelines established by the committee and international standards for animal welfare (approval ID: SCAU#2021c008). We made every effort to reduce the suffering of animals.

### Experimental animals and tissues

Four 7-week-old Xinghua female chickens were received from the Zhicheng Poultry Breeding Co., Ltd. (Guangdong, China). The tissues (including the cerebrum, cerebellum, hypothalamus, heart, liver, spleen, lung, kidney, muscular stomach, glandular stomach, breast muscle, and leg muscle) were collected, quickly frozen into liquid nitrogen, and then stored at  $-80^{\circ}\text{C}$ .

### Cell culture and transfection

CPMs were isolated from E11 chicken leg muscles as previously described [19] and cultured in Roswell Park Memorial Institute (RPMI)-1640 medium (Gibco, USA) with 20% fetal bovine serum (Gibco). All transient transfections were performed using Lipofectamine 3000 reagent (Invitrogen, USA) according to the manufacturer’s instructions.

### Lentivirus assay

Chinese native breeds (XH chickens) were used for the in vivo experiment in this study. For the construction of animal models of *LncRNA-TBP* overexpression and knockdown.

1-day-old chicks were randomly divided into two groups (Lv-*LncRNA-TBP* and Lv-NC;  $n=30$ ), respectively. Chicks received two intramuscular doses of lentivirus ( $10^6$  titers) in two different sites of the gastrocnemius. Thirteen days after the initial injection, chick gastrocnemius samples were collected from the above two groups.

7-days-old chickens were randomly divided into two groups (Chol-ASO-*LncRNA-TBP* and Chol-ASO-NC;  $n=15$ ) respectively. Chicks received two intramuscular doses of modified ASOs (40 nmol) by intramuscular injection on days 14 and 18. The chickens were euthanized at 21 days old, and the gastrocnemius muscles were detached and stored at  $-80^{\circ}\text{C}$ .

### Rapid-amplification of cDNA ends (RACE)

The full-length of *LncRNA-TBP* was amplified by using a SMARTer RACE cDNA Amplification Kit (Clontech, Japan), following the manufacturer’s instructions. The primer pairs used in RACE are listed in Additional file 10: Table S4.

### RNA isolation, complementary DNA (cDNA) synthesis, and real-time (RT) PCR analysis

Total RNA was extracted from tissues or cells using RNAiso plus reagent (TaKaRa, Japan). cDNA synthesis was obtained by using a PrimeScript RT Reagent Kit with gDNA Eraser (Perfect Real Time) (Takara, Japan). Real-time quantitative PCR (qRT-PCR) reactions were performed on a QuantStudio 5 Real-Time PCR

Systems (Thermo Fisher, Waltham, MA, USA) by using an ChamQ Universal SYBR qPCR Master Mix (Vazyme, China). All primers for RT-PCR and real-time qPCR are listed in Additional file 10: Table S4.

#### Plasmid construction and RNA oligonucleotides

For Flag fusion protein construction, twelve ORFs of *LncRNA-TBP* were amplified and cloned into pcDNA3.1-3xFlag (SiDanSai, Shanghai, China), and pcDNA3.1-3xFlag- $\beta$ -actin was used as a positive control.

For overexpression vectors construction, the full-length sequence of *LncRNA-TBP* was amplified and cloned into reconstructive pcDNA3.1 vector (Promega, Madison, WI, USA), which with GFP tag at the C-terminus.

For viral vectors constructed, the full-length sequence of *LncRNA-TBP* was amplified and then cloned into the lentiviral vector (pLVX-mCMV-ZsGreen-IRES-Puro; Addgene, Cambridge, MA, USA).

The antisense oligonucleotide (ASO) with Cy3-modified that was used for the specific knockdown of *LncRNA-TBP* was designed and synthesized by Guangzhou RiboBio (Guangzhou, China). The siRNA against *TBP* (NCBI Reference Sequence: NM\_205103.1) was also designed and synthesized.

The primers and oligonucleotide sequences used in this study are shown in Additional file 10: Table S4 and S5.

#### Flow cytometry, 5-ethynyl-2'-deoxyuridine (EdU) and cell counting kit-8 (CCK-8) assays

The Cell Cycle Analysis Kit (Thermo Fisher Scientific, USA), C10310 EdU Apollo In Vitro Imaging Kit (RiboBio, China) and TransDetect Cell Counting Kit (TransGen, Beijing, China) were used for flow cytometry, EdU, and CCK-8 assay, as the manufacturer's protocol.

#### Immunofluorescence, immunohistochemistry and hematoxylin and eosin staining

Immunofluorescence was performed using anti-MyHC (B103; DSHB, USA; 2.5 mg/mL), and images were captured using a fluorescence microscope (DMI8; Leica, Germany). The area of cells labeled with anti-MyHC was measured and calculated as previously described [20].

Immunohistochemistry was carried out using an SP-POD Kit (SP0041; Solarbio, China) with primary antibodies including anti-MYH1A (F59, DSHB, 1:100) and anti-MYH7B (S58, DSHB, 1:300). The number of myofibers labeled with anti-MYH1A or anti-MYH7B was calculated.

Hematoxylin and eosin (H&E) staining was performed using muscle tissues embedded in paraffin and cut into 4-mm-thick transverse sections. Subsequently, the sections were stained with H&E.

#### Mitochondrial DNA (mtDNA) content and fatty acid oxidation (FAO) rate assay

Total DNA was extracted using the Tissue DNA Kit (D3396, Omega, GA, USA) according to the manufacturer's instructions. The amount of mitochondrial DNA was determined by quantification of cytochrome c oxidase subunit II (COX2). The nuclear-encoded  $\beta$ -globin gene was used as an internal control. Primers used in this study can be found in Additional file 10: Table S4.

The mitochondria of the myoblast and gastrocnemius were isolated using the Cell/Tissue Mitochondria Isolation Kit (C3601/C3606, Beyotime, China). After measuring the mitochondrial protein concentration, freshly isolated mitochondria were subjected to FAO rate assay with the Colorimetric Fatty Acid Oxidation Rate Assay Kit (HL50679, Haling, Shanghai, China), according to the manufacturer's protocol.

#### Metabolite and enzyme activities assays

Content of TG, FFA, and glycogen as well as enzyme activity of LDH and SDH in skeletal muscle were measured using commercially available kits (BC0625, BC0595, BC0345, BC0685, BC0955, respectively; Solarbio, China), according to the manufacturer's instructions.

#### Central carbon metabolic profiling

*LncRNA-TBP* overexpression gastrocnemius samples (n=6) were used for metabolites extraction and then performed on HPIC-MS/MS analysis. The high-performance ion-exchange liquid chromatography (HPIC) separation was carried out using a Thermo Scientific Dionex ICS-6000 HPIC System (Thermo Fisher Scientific, IL, USA). An AB SCIEX 6500 QTRAP+ triple quadrupole mass spectrometer (AB Sciex, USA), equipped with electrospray ionization (ESI) interface, was applied for assay development.

Metabolic hierarchical clustering analysis (HCA) was performed using Cluster3.0 software as previously described [21].

#### Western blot analysis

Western blot analysis was performed as previously described [44]. The primary antibodies used were anti-FLAG (AF519, Beyotime, 1:1,000), anti-MYOD (ABP53067, Abbkine, 1:500), anti-MyHC (B103, DSHB, 0.5 mg/mL), anti-FASN (10624-2-AP, Proteintech, 1:200), anti-CPT1 (bs-23779R, Bioss, 1:500), anti-ULK1 (bs-3602R, Bioss, 1:500), anti-LC3B (NB100-2220, Novus, 2.0 mg/mL), anti-P62 (18420-1-AP, Proteintech, 1:1,000), anti-TBP (44059, Cell signaling, 1:1000), anti-KLF4 (bs-1064R, Bioss, 1:500), anti-GPI (GTX113203, GeneTex, 1:500), anti-TNNI2 (bs-10617R, Bioss, 1:500), anti-CDKN1A (GTX112898, GeneTex, 1:500), and anti-GAPDH (60004-1-Ig, Proteintech, 1:5,000). ProteinFind

goat anti-mouse IgG(H+L), HRP conjugate (HS201-01, TransGen, 1:1,000) and ProteinFind goat anti-rabbit IgG(H+L), HRP conjugate (HS101-01, TransGen, 1:500) were used as secondary antibodies. The original images of western blot are shown in Additional file 1.

#### RNA pull-down assay and RIP assay

Biotinylated RNAs were harvested by using a Ribo RNAmax-T7 biotin-labeled transcription kit (RiboBio, China). A Pierce Magnetic RNA-Protein Pull-Down Kit (Thermo Fisher Scientific) was used in RNA-protein pull-down experiments according to the manufacturer's instructions. The eluted products were identified by mass spectrometry with a Q Exactive mass spectrometer (Thermo Fisher) or western blot.

Immunoprecipitation Kit (Millipore, USA) according to the manufacturer's instructions. The antibody used for RIP assays was anti-TBP (44059, Cell Signaling, 1:100).

#### Chromatin immunoprecipitation (CHIP)

TBP ChIP was performed with ChIP Kit (Millipore, Bedford, MA) according to the manufacturer's instructions. Briefly, the ChIPed DNA was eluted, reverse X-linked, purified, and analyzed by qRT-PCR. All primers used in ChIP-qPCR are presented in Additional file 10: Table S4.

#### Luciferase reporter assay

For luciferase reporter assay, reporter plasmids with the promoter region of *KLF4*, *GPI*, *TNNI2*, and *CDKN1A* were transfected into CPMs by Lipofectamine 3000 (Invitrogen, USA) in 96-well plates. The luciferase activities were measured 48 h after differentiation by using Dual-Luciferase<sup>®</sup> Reporter Assay System (Promega, Madison, WI, USA). Firefly activity was normalized to Renilla luciferase activity.

#### Statistical analysis

In this study, all experiments were repeated at least three times, and results were represented as mean  $\pm$  SEM. Where applicable, the statistical significance of the data was tested using independent sample *t*-test or ANOVA followed by Dunnett's test. The types of tests and the *P*-values, when applicable, are indicated in the figure legends.

## Results

### *LncRNA-TBP* is a novel lncRNA associated with myogenesis

Our previous RNA-seq study found a muscle-related lncRNA (*LncRNA-TBP*) was highly expressed in SOL (Fig. 1A, B). 5' and 3' ends of *LncRNA-TBP* were identified by RACE analysis (Fig. 1C). The NCBI BLAST indicated that *LncRNA-TBP* located on Chromosome 3 and spanned from 82341588 to 82342330, and 82369736 to 82370049 with 1057 nt long, relatively conserved in *Meleagris gallopavo*, *Apteryx mantelli mantelli*, and

*Numida meleagris* (Additional file 2: Fig. S1 and Additional file 10: Table S1). *LncRNA-TBP* highly expressed in polyadenylated RNA (Fig. 1D). *LncRNA-TBP* upregulated during myogenic differentiation, and enriched in leg muscles and breast muscles (Fig. 1E, F), implying that it may play an important role in skeletal muscle development. In addition, cell-fractionation assays demonstrated that *LncRNA-TBP* is mainly present in the nucleus of chicken primary myoblasts (CPMs) (Fig. 1G). To further prove the coding potential of *LncRNA-TBP*, we analyzed the twelve potential ORFs of *LncRNA-TBP* by western blot. The results show that *LncRNA-TBP* is a lncRNA without protein-encoding potential (Fig. 1H).

### *LncRNA-TBP* inhibits myoblast proliferation and promotes myoblast differentiation

*LncRNA-TBP* was predominantly expressed in breast muscle and leg muscle (Fig. 1F), implying that *LncRNA-TBP* plays an important role in myogenesis. To assess the effect of *LncRNA-TBP* on proliferation and differentiation of myoblast, the overexpression vector and inhibitor of *LncRNA-TBP* were transfected into CPMs (Fig. 2A and Additional file 3: Fig. S2A). Overexpression of *LncRNA-TBP* increased the expression of cell cycle-inhibiting genes like *CDKN1A* and *CDKN1B* while decreasing the expression level of cell cycle-promoting genes like *PCNA*. The opposite result was observed with *LncRNA-TBP* knockdown (Fig. 2B and Additional file 3: Fig. S2B). The 5-ethynyl-2'-deoxyuridine (EdU) staining and cell counting kit-8 (CCK-8) assay demonstrated that *LncRNA-TBP* overexpression significantly inhibited myoblast proliferation and viability (Fig. 2C–E). Conversely, interference with *LncRNA-TBP* promoted EdU incorporation and myoblast proliferation (Additional file 3: Fig. S2C–E). At the same time, overexpression of *LncRNA-TBP* significantly increased the number of G0/G1 cells, and the number of S phase cells was lower than the control group, whereas myoblast division was inhibited with *LncRNA-TBP* interference (Fig. 2F and Additional file 3: Fig. S2F).

To further investigate the potential function of *LncRNA-TBP* in myoblast differentiation, immunofluorescence staining was performed after overexpression and inhibition of *LncRNA-TBP*. The results showed that overexpression of *LncRNA-TBP* increased the total areas of myotubes, while myotube formation was facilitated (Fig. 2G–I). In contrast, *LncRNA-TBP* interference suppressed myoblast differentiation (Additional file 3: Fig. S2G–I). Moreover, the expressions level of myoblast differentiation marker genes, including *MYOD*, *MYOG*, and *MyHC* were significantly upregulated with *LncRNA-TBP* overexpression (Fig. 2J, K). Conversely, *LncRNA-TBP* interference repressed their expression (Additional file 3: Fig. S2J, K).

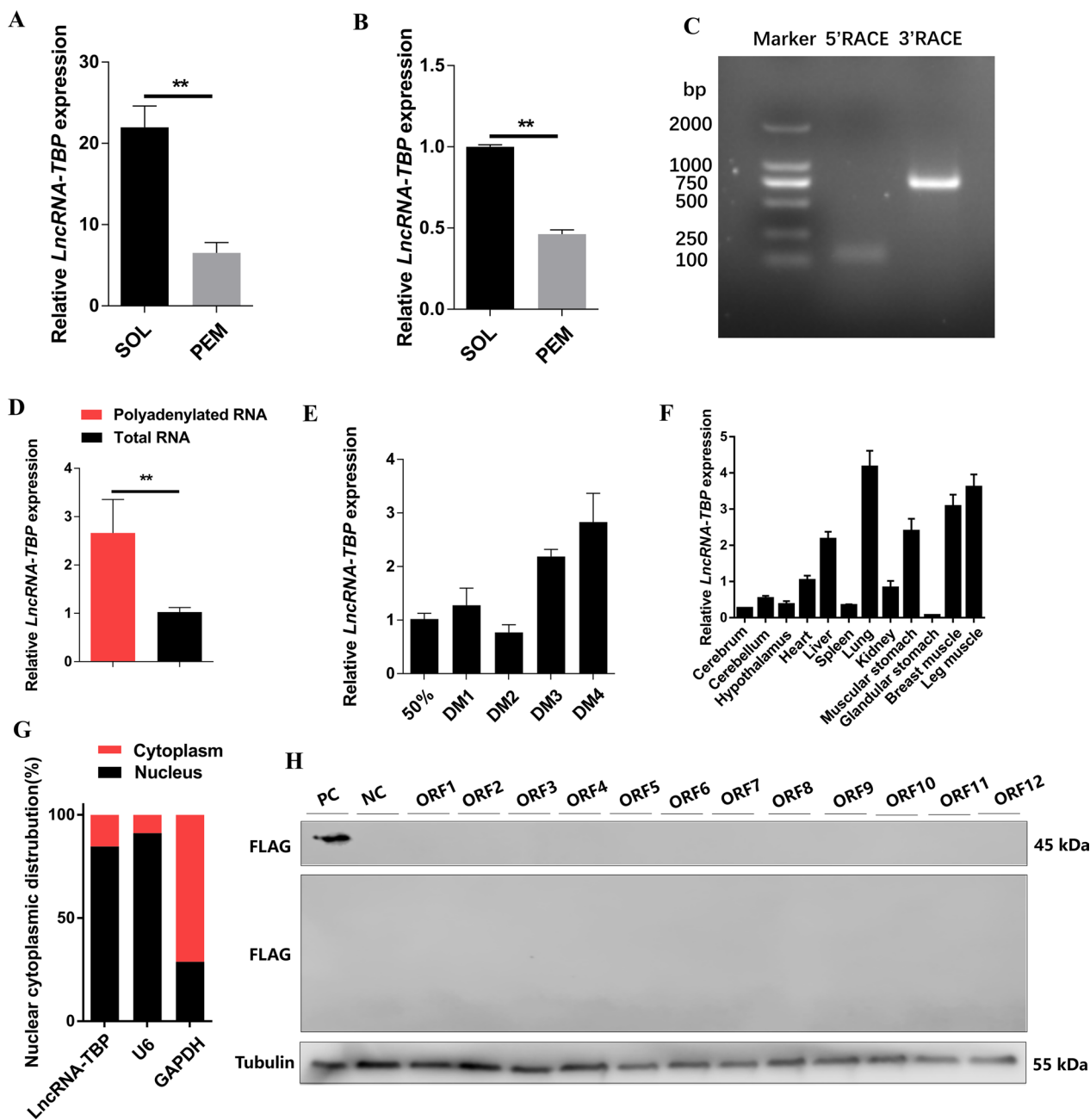


**Fig. 1** Identification of *LncRNA-TBP*. **A** *LncRNA-TBP* expression of pectoralis major and soleus of 7-week-old Xinghua chickens by RNA-seq (n = 4). **B** Relative *LncRNA-TBP* expression of pectoralis major and soleus of 7-week-old Xinghua chickens by qRT-PCR (n = 4). **C** Results of *LncRNA-TBP* 5' RACE and 3' RACE. **D** Relative *LncRNA-TBP* expression in polyadenylated RNA and total RNA (n = 4). **E** Relative *LncRNA-TBP* expression during CPMs proliferation and differentiation (n = 3). **F** Tissues expression profiles of *LncRNA-TBP*. The horizontal axis and vertical axis indicate different tissues and their relative expression values, respectively (n = 3). **G** The distribution of *LncRNA-TBP* in the cytoplasm and nuclei of CPMs was determined by qRT-PCR. GAPDH and U6 serve as cytoplasmic and nuclear localization controls, respectively. **H** Western blot analysis of the coding ability of *LncRNA-TBP*. The potential ORFs of *LncRNA-TBP* were cloned into the pcDNA3.1-3xFlag-C vector. CPMs transfected with  $\beta$ -actin were used as a positive control (PC) and untransfected CPMs were used as a negative control (NC). Results are presented as mean  $\pm$  SEM. In panels (A, B and D), the statistical significance of differences between means was assessed using independent sample *t*-test. (\**P* < 0.05; \*\**P* < 0.01)

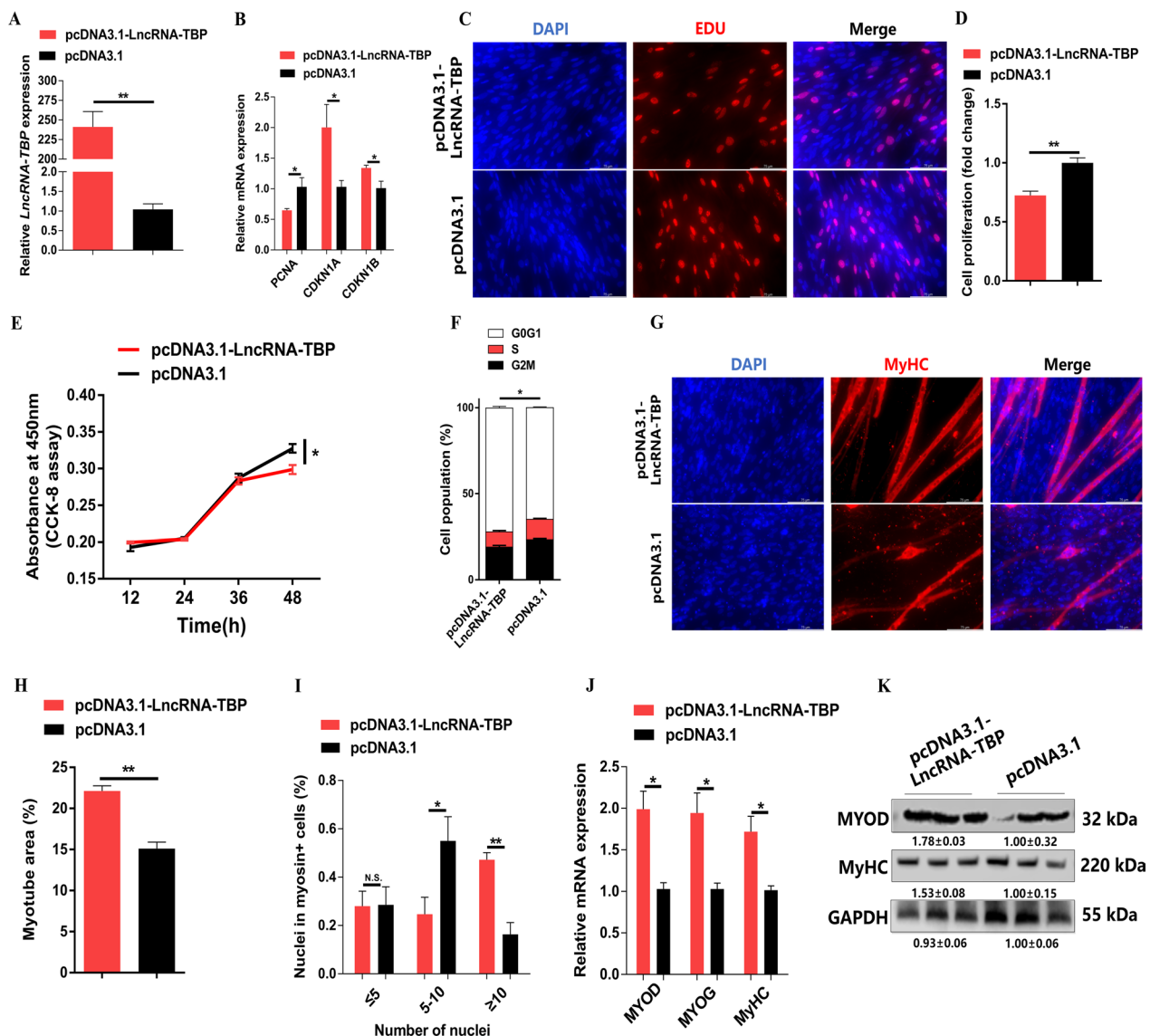


**Fig. 2** *LncRNA-TBP* inhibits myoblast proliferation but promotes myogenic differentiation. **A** Relative *LncRNA-TBP* expression with *LncRNA-TBP* overexpression in vitro (n = 6). **B** Relative mRNA levels of several cell cycle genes with overexpression of *LncRNA-TBP* (n = 6). **C** The proliferation of transfected CPMs was assessed by 5-ethynyl-2'-deoxyuridine (EdU) incorporation (n = 3). **D** The proliferation rate of myoblasts after the overexpression of *LncRNA-TBP* (n = 8). **E** CCK-8 assays were performed in CPMs with *LncRNA-TBP* overexpression (n = 6). **F** Cell cycle analysis of myoblasts after the overexpression of *LncRNA-TBP* (n = 4). **G-I** MyHC immunostaining (n = 3) (**G**), myotube area (%) (n = 8) (**H**) and myoblast fusion index (n = 8) (**I**) of CPMs transfected with *LncRNA-TBP* overexpression. Cells were differentiated for 72 h after transfection. **J** and **K** Relative mRNA (n = 6) (**J**) and protein (n = 3) (**K**) expression levels of myoblast differentiation marker genes with *LncRNA-TBP* overexpression. In panel **H**, the numbers shown below the bands were folds of band intensities relative to control. Band intensities were quantified by ImageJ and normalized to GAPDH. Data are expressed as a fold-change relative to the control. Results are shown as mean ± SEM. In panels (**A**, **B**, **D-F** and **H-J**), the statistical significance of differences between means was assessed using an independent sample *t*-test. (\**P* < 0.05; \*\**P* < 0.01; N.S., no significant difference)

***LncRNA-TBP* accelerates fatty acid oxidation, and enhances TCA cycle flux in skeletal muscle**

To verify whether *LncRNA-TBP* regulates skeletal muscle development in vivo, lentiviral-mediated *LncRNA-TBP* overexpression (LV-*LncRNA-TBP*) or cholesterol-modified antisense oligonucleotide

(Chol-ASO-*LncRNA-TBP*) were injected to the gastrocnemius of Xinghua chicken (Fig. 3A and Additional file 4: Fig. S3A). *LncRNA-TBP* overexpressed increased mitochondrial DNA content, which potentially contributed to the acceleration of fatty acid oxidation (FAO) and inhibited the accumulation of free

fatty acid (FFA) and triglyceride (TG) (Fig. 3B–D). In contrast, mitochondrial DNA content and fatty acid  $\beta$ -oxidation were reduced after the *LncRNA-TBP* knockdown (Additional file 4: Fig. S3B–D). Besides, the qPCR and western blotting analyses showed that knockdown of *LncRNA-TBP* downregulated FAO-related genes like *CPT1* and upregulating key genes involved in fatty acid synthesis (such as *FASN*), while opposite results were shown with *LncRNA-TBP* overexpression (Fig. 3E, F and Additional file 4: Fig. S3E, F).

Mitochondria switch between lipid and glucose oxidation through the TCA cycle to generate ATP, which is pivotal for maintaining systemic energy homeostasis [19–22]. Given that overexpression of *LncRNA-TBP* promoted the content of mitochondrial DNA (Fig. 3B), we performed a comparative metabolome analysis to study whether *LncRNA-TBP* functions muscle metabolism. The result of hierarchical clustering analysis (HCA) separated controls and overexpression of *LncRNA-TBP* (Fig. 3G and Additional file 11: Table S2). For example, compared with control, glycolytic metabolites such as fructose 6-phosphate and glucose 6-phosphate were significantly decreased with *LncRNA-TBP* overexpression (Fig. 3H and Additional file 11: Table S2). In the meantime, metabolites of the TCA cycle, including malic acid, isocitric acid, and fumaric acid were significantly promoted (Fig. 3H and Additional file 11: Table S2). Altogether, our results indicated that *LncRNA-TBP* decreases the end products of glycolysis and elevates metabolites of the TCA cycle by promoting mitochondrial function, leading to reduction of lipid accumulation.

### ***LncRNA-TBP* activates slow-twitch muscle phenotype and induces muscle hypertrophy**

Skeletal muscle development is primarily regulated by fiber type composition and muscle fiber size. The composition of myofiber types is closely related to the way muscles are metabolized [23, 24]. Given that *LncRNA-TBP* is highly expressed in SOL and mediated the flux of glycolysis and TCA cycle, we further examined whether *LncRNA-TBP* could affect the conversion of skeletal

muscle fiber types in vivo. As expected, the activity of lactate dehydrogenase (LDH) was suppressed, while the activity of succinate dehydrogenase (SDH) was enhanced with *LncRNA-TBP* overexpression (Fig. 4A). Meanwhile, glycogen content was increased and expression of glycolytic and glycolytic genes was downregulated with overexpression of *LncRNA-TBP* (Fig. 4B, C). The opposite results were shown with the knockdown of *LncRNA-TBP* (Additional file 5: Fig. S4A–C). The expression levels of fast-twitch myofiber genes like *SOX6* and slow-twitch myofiber genes (such as *TNNC1*, *TNNI1* and *TNNT1*) were further tested. It was found that overexpression of *LncRNA-TBP* promoted expressions of slow-twitch myofiber genes (Fig. 4D). More importantly, results of immunohistochemistry showed that *LncRNA-TBP* overexpression promoted the expression level of MYH7B/slow-twitch protein and suppressed the expression level of MYH1A/fast-twitch protein (Fig. 4E, F). On the contrary, *LncRNA-TBP* knockdown upregulated the fast-twitch protein level and drove the transformation of slow-twitch to fast-twitch myofibers (Additional file 5: Fig. S4D–F).

Recent evidences have revealed that remodeling of skeletal muscle fiber types can affect muscle mass, and induce muscle hypertrophy and muscle atrophy by anabolic and catabolic signaling pathways, respectively [25]. *LncRNA-TBP* overexpression leads to increased muscle mass and cross-sectional area (CSA), while the opposite result occurred upon *LncRNA-TBP* knockdown (Fig. 3G and H and Additional file 5: Fig. S4G, H), suggesting that *LncRNA-TBP* regulates skeletal muscle hypertrophy. Autophagy is a highly conserved homeostatic process carrying out degradation of cytoplasmic components including damaged organelles, toxic protein aggregates, and intracellular pathogen [26]. Maintaining basal autophagy flux is essential to clear damaged organelles or recycle macromolecules in muscles during metabolic stress [27]. To further explore the regulatory mechanism of *LncRNA-TBP* in inducing muscle hypertrophy, we detected expressions of autophagy-related genes. *LncRNA-TBP* overexpression upregulated the expression level of *SQSTM1*, whereas expressions

(See figure on next page.)

**Fig. 3** *LncRNA-TBP* promotes fatty acid oxidation and TCA cycles in skeletal muscle. **A** Relative *LncRNA-TBP* expression in gastrocnemius after infected with lentivirus-mediated *LncRNA-TBP* overexpression (Lv-*LncRNA-TBP*) or negative control (Lv-NC) (n = 4). **B** Relative mtDNA content in *LncRNA-TBP* overexpression gastrocnemius (n = 4). **C** Relative fatty acid  $\beta$ -oxidation rate with overexpression of *LncRNA-TBP* in gastrocnemius (n = 4). **D** Relative free fatty acid (FFA) and triglyceride (TG) content in gastrocnemius with *LncRNA-TBP* overexpression (n = 4). **E** and **F** Relative mRNA (n = 6) (**E**) and protein (n = 3) (**F**) expression levels of fatty acid oxidation or synthesis related-genes in gastrocnemius with *LncRNA-TBP* overexpression. **G** Hierarchical clustering analysis (HCA) of metabolites in gastrocnemius with overexpression of *LncRNA-TBP* (n = 6). The colors indicate the relative levels in the overexpression of *LncRNA-TBP* or control group. **H** Relative metabolite content of glycolysis and tricarboxylic acid (TCA) cycle in gastrocnemius with *LncRNA-TBP* overexpression (n = 6). In panel **F**, the numbers shown below the bands were folds of band intensities relative to control. Band intensities were quantified by ImageJ and normalized to GAPDH. Data are expressed as a fold-change relative to the control. Results are shown as mean  $\pm$  SEM. In panels (**A–E** and **H**), the statistical significance of differences between means was assessed using an independent sample t-test. (\* $P < 0.05$ ; \*\* $P < 0.01$ ; N.S., no significant difference)

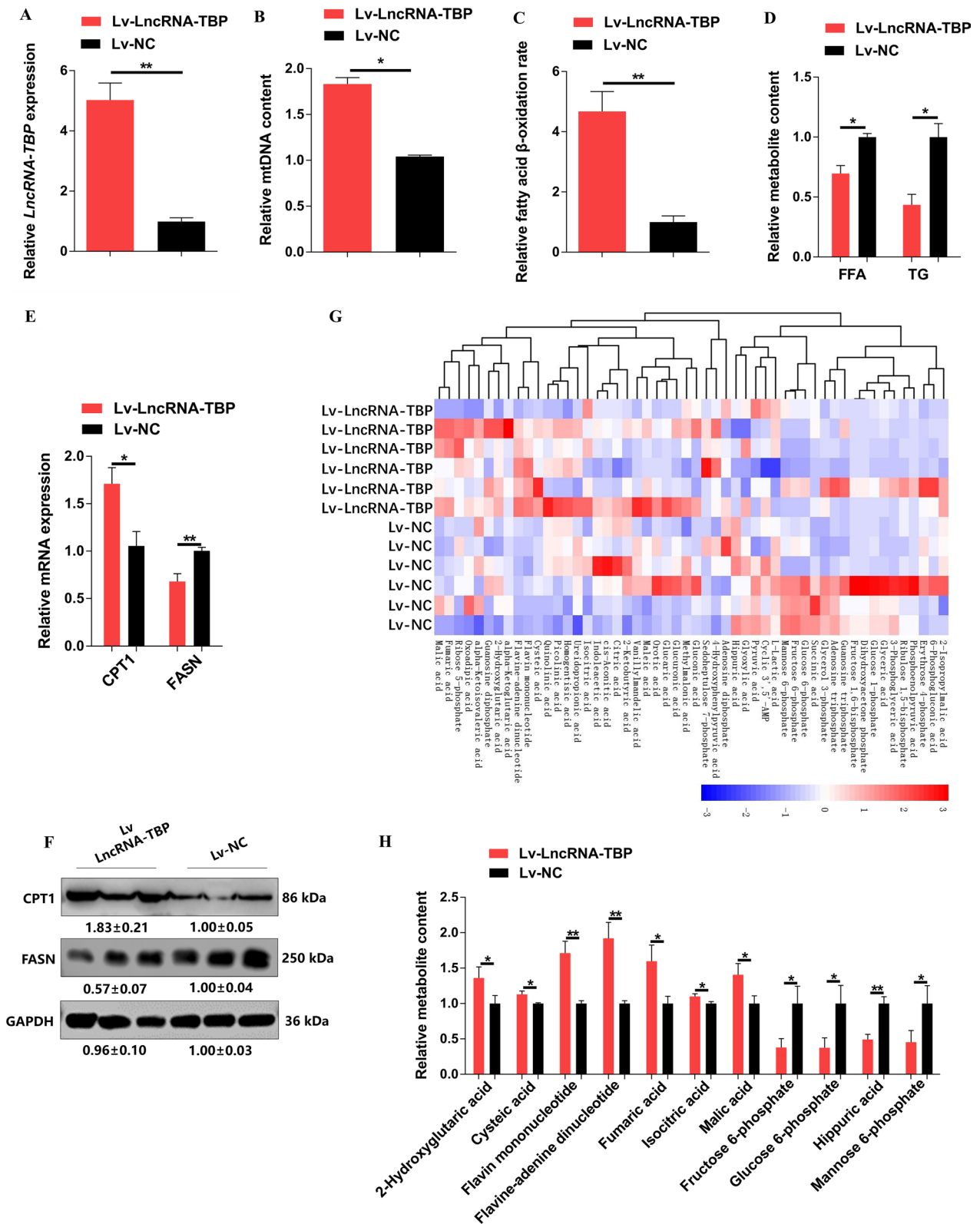


**Fig. 3** (See legend on previous page.)



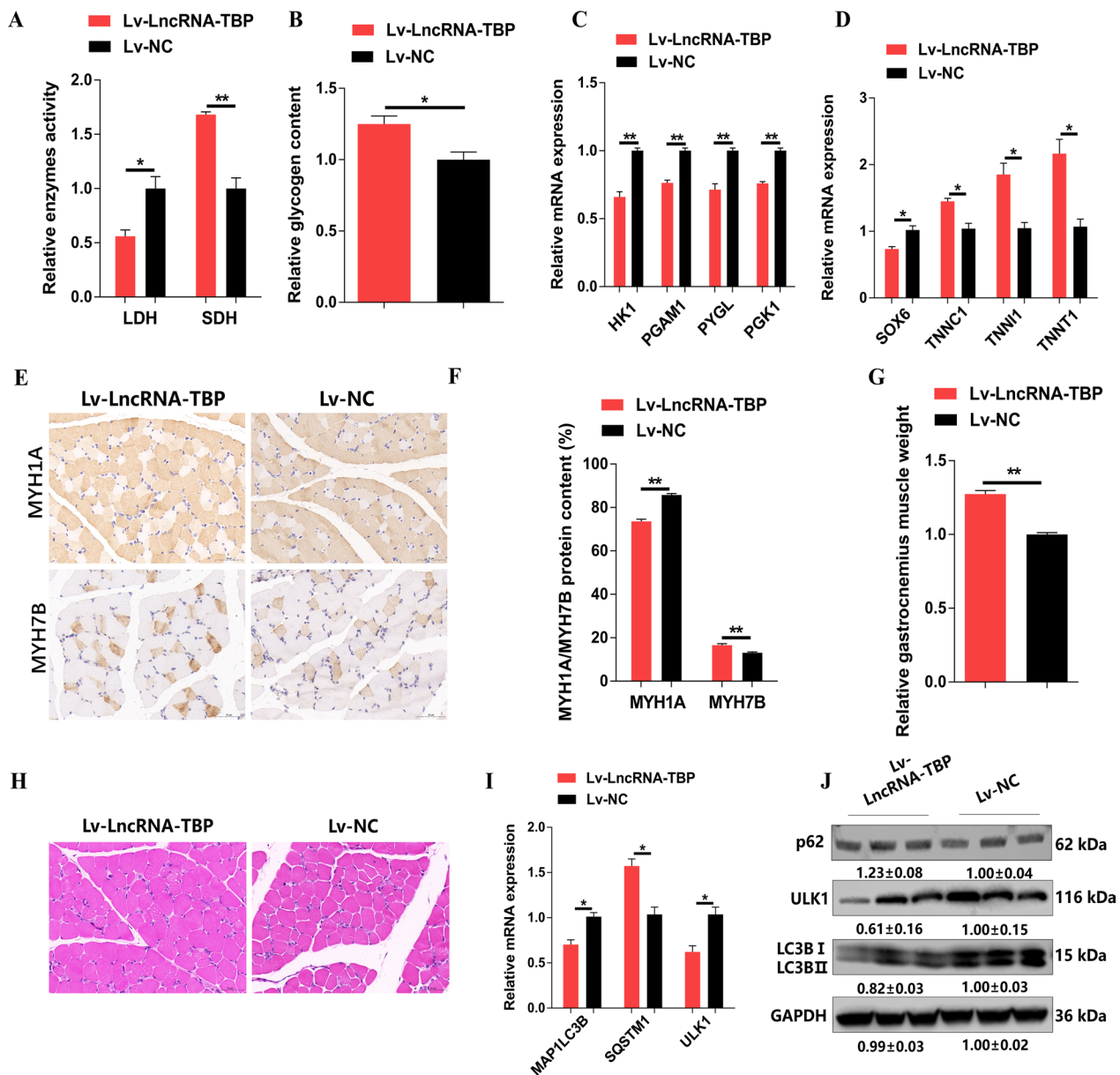


**Fig. 4** *LncRNA-TBP* activates slow-twitch muscle phenotype and induce muscle hypertrophy. **A** Relative enzymes activity of lactic dehydrogenase (LDH) and succinate dehydrogenase (SDH) in gastrocnemius infected with *LncRNA-TBP* overexpression (n = 4). **B** Relative glycogen content in *LncRNA-TBP* overexpression gastrocnemius (n = 5). **C** Relative mRNA expression levels of glycogenolytic and glycolytic genes in *LncRNA-TBP* overexpression gastrocnemius (n = 6). **D** Relative mRNA expression levels of several fast-/slow-twitch myofiber genes in overexpression of *LncRNA-TBP* gastrocnemius (n = 6). **E** and **F** Immunohistochemistry analysis of MYH1A/MYH7B (n = 3) (**E**) and MYH1A/MYH7B protein content (n = 8) (**F**) in gastrocnemius with *LncRNA-TBP* overexpression. **G** Relative gastrocnemius muscle weight after infected with lentivirus-mediated *LncRNA-TBP* overexpression (n = 6). **H** H&E staining in overexpression of *LncRNA-TBP* gastrocnemius (n = 3). **I** and **J** Relative mRNA (n = 6) (**I**) and the protein (n = 3) (**J**) expression levels of the autophagy-related genes in gastrocnemius with *LncRNA-TBP* overexpression. In panel **J**, the numbers shown below the bands were folds of band intensities relative to control. Band intensities were quantified by ImageJ and normalized to GAPDH. Data are expressed as a fold-change relative to the control. Results are shown as mean ± SEM. In panels **A–D**, **F** and **H–I**, the statistical significance of differences between means was assessed using an independent sample t-test. (\**P* < 0.05; \*\**P* < 0.01; N.S., no significant difference)

of autophagy-related genes (such as *MAP1LC3B*, and *ULK1*) and content of LC3BII were downregulated (Fig. 4I, J). Conversely, *LncRNA-TBP* knockdown

activated autophagy (Additional file 5: Fig. S4I, J), suggesting that *LncRNA-TBP* may promote muscle hypertrophy by decreasing basal autophagy flux.

**LncRNA-TBP directly interacts with TBP**

Recent studies have found that many nuclear lncRNAs perform their functions through interaction with proteins [28]. The nuclear localization of *LncRNA-TBP* suggested that this lncRNA may modulates the transcriptional regulation of target genes. Thus, we attempted to identify the protein partners of *LncRNA-TBP*. First, the potential *LncRNA-TBP*-binding proteins were predicted using the RNA-protein interaction prediction (RPISeq), and TBP was found may interact with *LncRNA-TBP* (Additional file 6: Fig. S5A). To validate this interaction between *LncRNA-TBP* and TBP, we performed

a RNA immunoprecipitation (RIP) analysis in CPMs. As expected, reverse transcription-polymerase chain reaction (RT-PCR) analysis of antibody-enriched RNA revealed that TBP antibody pulled down significantly more *LncRNA-TBP* than the IgG control (Fig. 5A), suggesting that TBP interacts with *LncRNA-TBP*. To determine the core protein-binding domain of *LncRNA-TBP*, we constructed a series of truncated *LncRNA-TBP* fragments. We found that like full-length *LncRNA-TBP*, all of the truncated fragments could physically bind TBP (Fig. 5B, C). Collectively, these findings showed that *LncRNA-TBP* directly interacts with TBP.

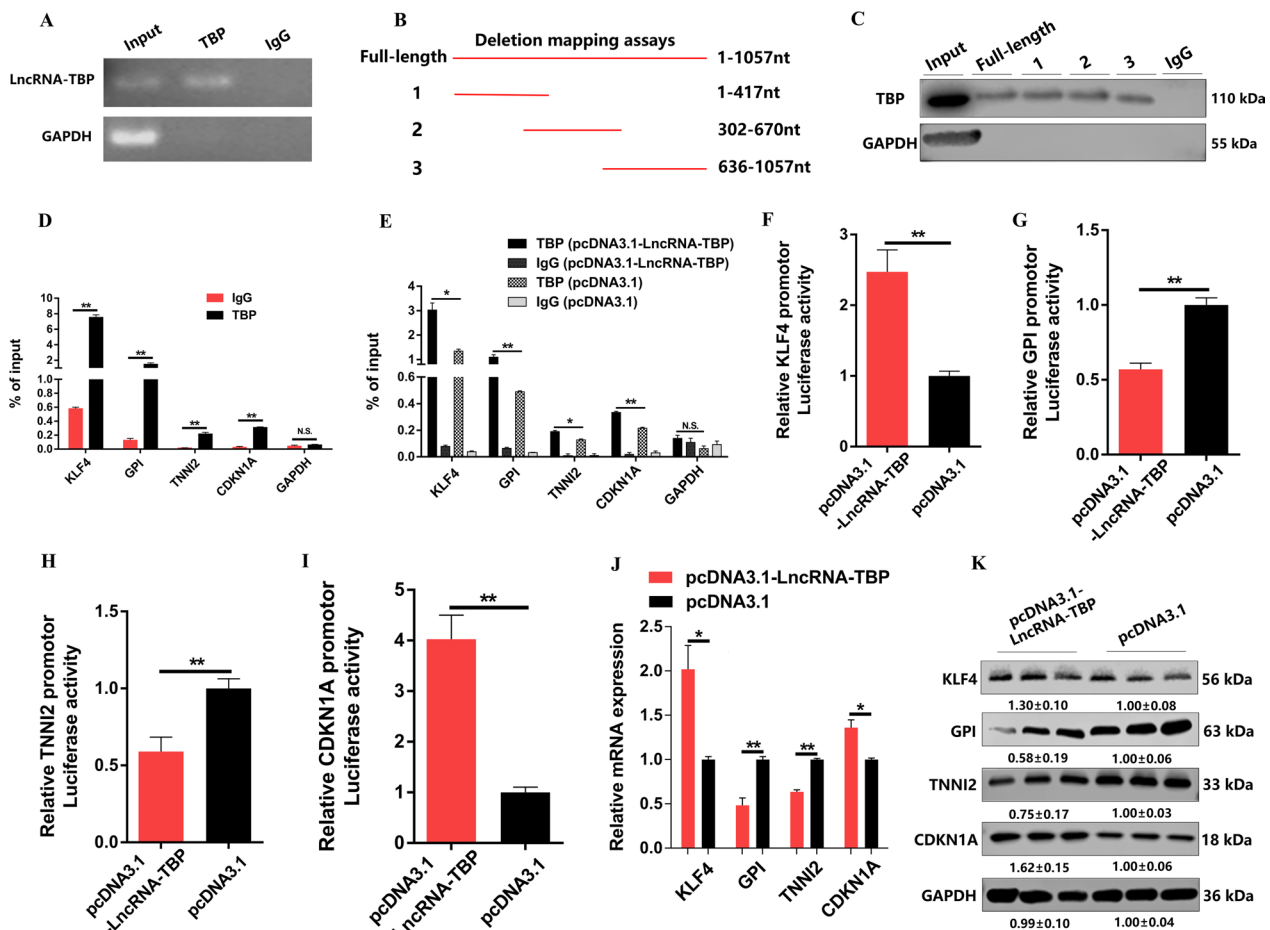


**Fig. 5** *LncRNA-TBP* interacts with TBP to regulate the transcriptional activity of TBP-target genes. **A** *LncRNA-TBP* interacts with TBP protein were determined by RNA Immunoprecipitation (RIP). **B** and **C** The interaction of full-length and truncated *LncRNA-TBP* (base pairs 1-417, 302-670 and 636-1057) (**B**) with TBP protein was determined by RNA pulldown (**C**). **D** ChIP-qPCR results showing that TBP enrichment at the *KLF4*, *GPI*, *TNNI2*, and *CDKN1A* promoters in CPMs (n = 3). **E** ChIP-qPCR results showing that *LncRNA-TBP* overexpression significantly increased TBP enrichment at the *KLF4*, *GPI*, *TNNI2*, and *CDKN1A* promoters in CPMs (n = 3). **F-I** The luciferase activities of the reporter show that the relative promoter activity of *KLF4* (**F**), *GPI* (**G**), *TNNI2* (**H**), and *CDKN1A* (**I**) significantly changed with *LncRNA-TBP* overexpression in CPMs (n = 6). **J-K** The relative mRNA (n = 4) (**J**) and protein (n = 3) (**K**) expression levels of *KLF4*, *GPI*, *TNNI2*, and *CDKN1A* after *LncRNA-TBP* overexpression. In panels **A**, **C**, and **K**, the numbers shown below the bands were folds of band intensities relative to control. Band intensities were quantified by ImageJ and normalized to  $\beta$ -Tubulin. Data are expressed as a fold-change relative to the control. Results are presented as mean  $\pm$  SEM. In panels **D-J**, the statistical significance of differences between means was assessed using an independent sample *t*-test. (\**P* < 0.05; \*\**P* < 0.01; N.S., no significant difference)

### **LncRNA-TBP regulates transcriptional activity of TBP-target genes by binding to TBP**

The general transcription factor (TBP) is a key initiation factor involved in transcription by all three eukaryotic RNA polymerases, is required for every single transcription event in eukaryotes [29–32]. Through our previous ATAC sequencing analysis, a total of 20 target genes (e.g., glycolysis-related genes (*GPI*), cell proliferation-related genes (*CDKN1A* and *KLF4*) and fast muscle-related genes (*TNNI2*)) were predicted be regulated by TBP (Additional file 6: Fig. S5B and Additional file 12: f S3). Gene ontology (GO) and Kyoto Encyclopedia of Genes and Genomes (KEGG) enrichment analysis found that these TBP-target genes were mainly enriched in biological processes such as cellular process, metabolic process, cellular component organization or biogenesis, and biological regulation, as well as participated in biological processes including metabolic pathways, carbon metabolism and so on (Additional file 6: Fig. S5C, D). By performing ChIP-qPCR, we validated that TBP can bind and regulate the promoter of *KLF4*, *GPI*, *TNNI2*, and *CDKN1A* (Fig. 5D).

Because *LncRNA-TBP* specifically interacts with TBP, we investigated whether there is a mutual regulation relationship between *LncRNA-TBP* and TBP in CPMs. The results showed that *LncRNA-TBP* knockdown or overexpression did not significantly influence TBP mRNA and protein expression (Additional file 7: Fig. S6A–D). These results suggested that *LncRNA-TBP* may regulate myogenesis through its interaction with TBP rather than by regulating TBP gene expression. Given that TBP functions in regulate the promoter activity of its target genes, we also performed ChIP-qPCR to elucidate whether *LncRNA-TBP* affects the capacity of TBP to bind the promoters of its target genes. *LncRNA-TBP* overexpression significantly increased the enrichment of TBP to the promoter of *KLF4*, *GPI*, *TNNI2*, and *CDKN1A*, whereas the results were reversed after *LncRNA-TBP* knockdown

(Fig. 5E and Additional file 8: Fig. S7A). Next, to determine whether *LncRNA-TBP* regulates promoter activity of TBP-target genes such as *KLF4*, *GPI*, *TNNI2*, and *CDKN1A*, luciferase reporter assays were performed. Overexpression of *LncRNA-TBP* promoted the promoter activity of *KLF4* and *CDKN1A* while inhibiting the promoter activity of *GPI* and *TNNI2* (Fig. 5F–I). Consistently, the knockdown of *LncRNA-TBP* had opposite effects in CPMs (Additional file 8: Fig. S7B–E). We further examined the mRNA and protein expressions of *KLF4*, *GPI*, *TNNI2*, and *CDKN1A*. As expected, *LncRNA-TBP* would promote the expression of *KLF4* and *CDKN1A*, while decreasing the expression of *GPI* and *TNNI2* (Fig. 5J, K and Additional file 8: Fig. S7F, G), suggesting that *LncRNA-TBP* can modulate transcriptional activity of TBP-target genes by binding to TBP protein.

### **TBP is involved in myogenesis**

TBP was upregulated during myoblast differentiation (Additional file 9: Fig. S8A), implying that it may play an important role in skeletal muscle development. Moreover, Subcellular location annotation showed that TBP protein exists in the nucleus (Additional file 9: Fig. S8B). To explore the potential biological functions of *TBP* in myogenesis, we examined the effects of *TBP* in myoblasts proliferation and differentiation in vivo. *TBP* was successfully overexpressed or knockdown in CPMs (Fig. 6A, L). Overexpression of *TBP* reduced cell-cycle-promoting genes while increasing the expression of cell-cycle-inhibiting genes. The EdU and CCK-8 assays showed that overexpression of *TBP* decreased EdU incorporation and repressed myoblast viability, whereas its inhibition promoted myoblast proliferation (Fig. 6B–E, N–P). Moreover, flow cytometric analysis revealed that *TBP* overexpression reduced the number of S-phase cells (Fig. 6F). Conversely, *TBP* inhibition resulted in a greater number of S-phase cells (Fig. 6Q).

(See figure on next page.)

**Fig. 6** *TBP* inhibits myoblast proliferation and promotes myogenic differentiation. **A** Relative *TBP* expression with *TBP* overexpression in vitro (n = 6). **B** Relative mRNA levels of several cell cycle genes with overexpression of *TBP* (n = 4). **C** The proliferation of transfected CPMs was assessed by 5-ethynyl-2'-deoxyuridine (EdU) incorporation (n = 3). **D** The proliferation rate of myoblasts after the overexpression of *TBP* (n = 8). **E** CCK-8 assays were performed in CPMs with *TBP* overexpression (n = 6). **F** Cell cycle analysis of myoblasts after the overexpression of *TBP* (n = 4). **G–I** MyHC immunostaining (n = 3) (**G**), myotube area (%) (n = 8) (**H**) and myoblast fusion index (n = 8) (**I**) of CPMs transduced with *TBP* overexpression. Cells were differentiated for 72 h after transfection. **J** and **K** Relative mRNA (n = 6) (**J**) and protein (n = 3) (**K**) expression levels of myoblast differentiation marker genes with *TBP* overexpression. **L** Relative *TBP* expression with *TBP* interference in vitro (n = 3). **M** Relative mRNA levels of several cell cycle genes with interference of *TBP* (n = 4). **N** The proliferation rate of myoblasts after the interference of *TBP* (n = 8). **O** The proliferation of transfected CPMs was assessed by 5-ethynyl-2'-deoxyuridine (EdU) incorporation (n = 3). **P** CCK-8 assays were performed in CPMs with *TBP* interference (n = 6). **Q** Cell cycle analysis of myoblasts after the interference of *TBP* (n = 4). **R–T** yotube area (%) (n = 8) (**R**), MyHC immunostaining (n = 3) (**S**) and myoblast fusion index (n = 8) (**T**) of CPMs transduced with *TBP* interference. Cells were differentiated for 72 h after transfection. **U** and **V** Relative mRNA (n = 6) (**U**) and protein (n = 3) (**V**) expression levels of myoblast differentiation marker genes with *TBP* interference. In panels **K** and **V**, the numbers shown below the bands were folds of band intensities relative to control. Band intensities were quantified by ImageJ and normalized to GAPDH. Data are expressed as a fold-change relative to the control. Results are shown as mean ± SEM. In panels **A**, **B**, **D–F**, **H–J**, **L–N**, **O–R** and **T**, **U**, the statistical significance of differences between means was assessed using an independent sample t-test. (\**P* < 0.05; \*\**P* < 0.01; N.S., no significant difference)

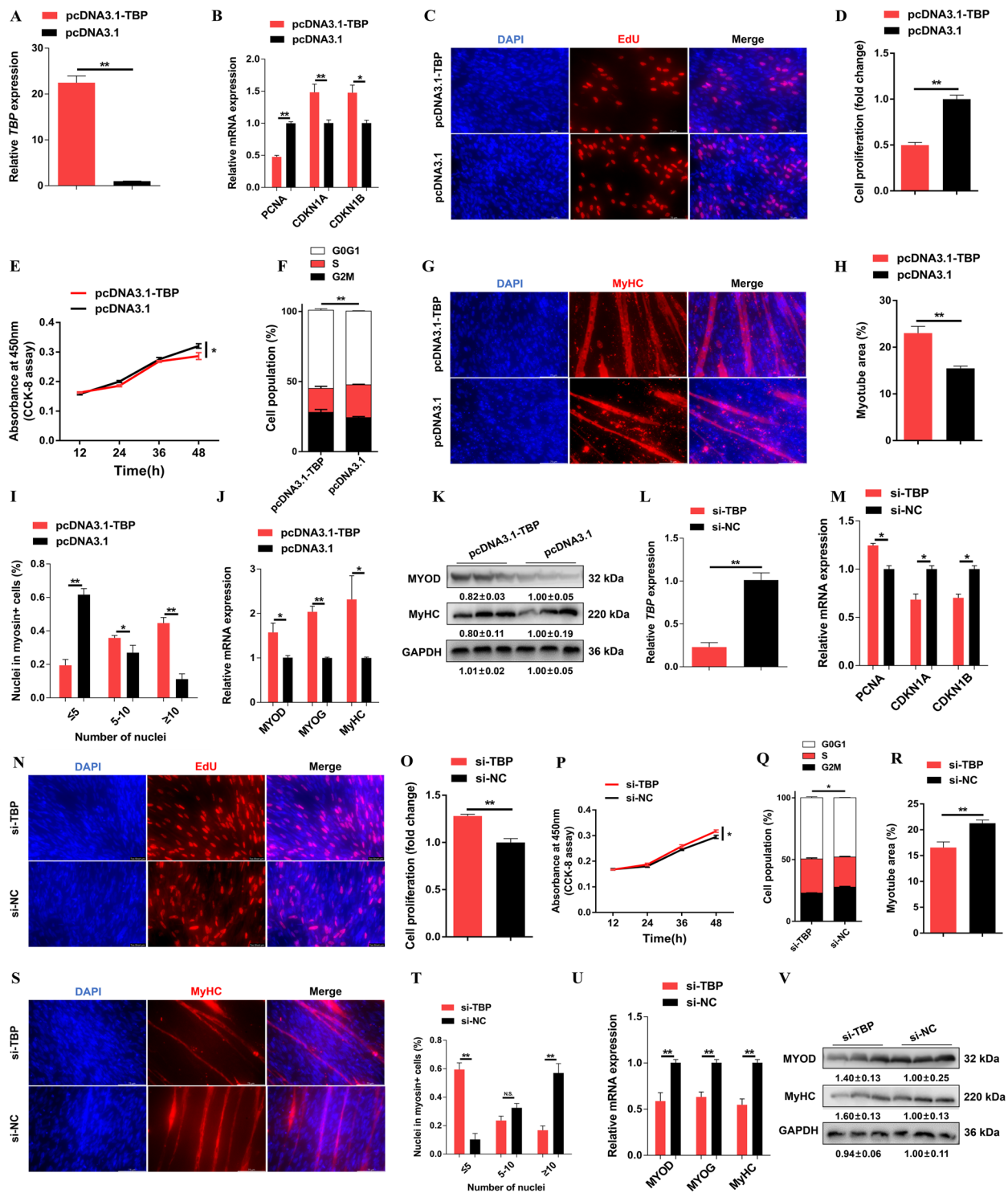


**Fig. 6** (See legend on previous page.)

Next, immunofluorescence staining was performed to detect the role of *TBP* in myogenic differentiation. *TBP* overexpression significantly facilitated myoblast differentiation, increased the total areas of myotubes and

myotube formation (Fig. 6G–I). Meanwhile, qPCR and western blotting showed that expressions of myoblast differentiation marker genes were upregulated with *TBP* overexpression (Fig. 6J, K). In contrast, *TBP* interference

repressed myoblast differentiation (Fig. 6R–V). Taken together, these data indicated that *TBP* suppresses myoblast proliferation and promotes myoblast differentiation, which is similar to *LncRNA-TBP* in function.

**Discussion**

Myogenesis is a highly ordered process including myoblast proliferation and differentiation, myotube formation and maturity, is controlled by a series of myogenic regulatory factors [33]. Many studies have suggested the important role of lncRNAs in skeletal muscle myogenesis while highlighting the necessity to systematically identify lncRNAs altered in skeletal muscle development [20, 34, 35]. The composition of myofiber types may influence meat quality by affecting the content of metabolites post-mortem in livestock such as pH, meat color, and drip loss [36, 37]. Compare to the fast-twitch muscle phenotype, the proportion of type slow-muscle fibers is proportional to the content of intramuscular fat, which have higher tenderness, flavor, and juiciness [38, 39]. Here, we found that *LncRNA-TBP* is highly expressed in skeletal muscle, and its expression gradually increased with the stage of myoblast differentiation. Functional analyses showed that *LncRNA-TBP* suppresses myoblast proliferation and induces myogenic differentiation in vivo, *LncRNA-TBP* activated the slow-twitch muscle phenotype and reduces fat deposition.

Skeletal muscle can maintain systemic energy homeostasis in response to various metabolic stresses through regulating glucose uptake, lipid storage, and energy balance [40]. In this study, we found that *LncRNA-TBP* increases cellular mitochondrial DNA content and facilitates fatty acid oxidation in skeletal muscle, resulting in inhibiting the deposition of intramuscular fat. In

the meantime, *LncRNA-TBP* reduced glycolytic capacity and increase oxidative capacity of skeletal muscle, which suppressed the autophagy pathway and reduced muscle atrophy.

TATA-binding protein (TBP) is a key component of the general transcription machinery that is involved in transcription by all three eukaryotic RNA polymerases [27–30]. Recent studies have found that mutant of TBP decreased its association with *MyoD*, which is a muscle-specific transcription factor, and caused a dramatic shrink in skeletal muscle mass [41, 42]. As a TATA-binding protein (TBP) associated factors, TAF9b was found can act a coactivator to stabilize the structure of P53 and promote P53 activation, thus reducing glycolysis, increasing superoxide levels, and inhibiting autophagy [12–15]. Notably, recent evidences have revealed that lncRNAs are able to be widely involved in a variety of biological processes through recruit RNA-binding proteins to regulate the transcription of target genes [43–45]. Here, we found *LncRNA-TBP* is a novel player in TBP-regulating network that can regulate the transcriptional activity of TBP-target genes by recruiting TBP protein, thus modulating myogenesis progression and inducing slow-twitch fibers.

**Conclusion**

In conclusion, we identify an lncRNA, *LncRNA-TBP*, and propose a mechanistic model to elucidate its role in the regulation of myogenesis and myofiber transformation through TBP-mediated transcriptional regulation (Fig. 7). Our findings present a novel model about the regulation of lncRNA in myogenesis, and will contribute to the development of further research.

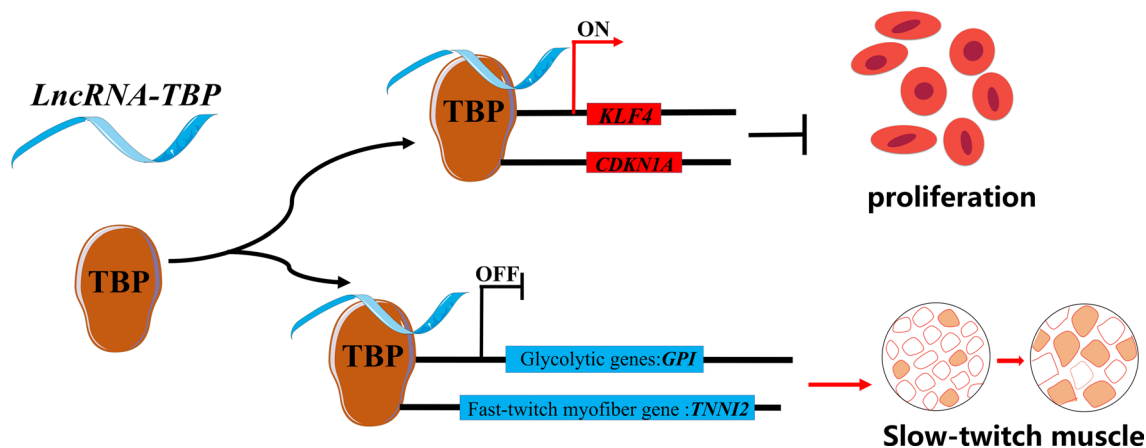


**Fig. 7** Model of *LncRNA-TBP* interacts with TBP to regulate the transcriptional activity of TBP-target genes, thus inhibiting myoblast proliferation, as well as activating slow-twitch muscle phenotype and inducing muscle hypertrophy

## Abbreviations

CPMs	Chicken primary myoblasts
CSA	Cross-section area
FAO	Fatty acid oxidation
FFA	Free fatty acid
HCA	Hierarchical clustering analysis
HE	Hematoxylin and eosin
LDH	Lactic dehydrogenase
mtDNA	Mitochondrial DNA
PEM	Pectoralis major
SDH	Succinate dehydrogenase
SOL	Soleus
TCA cycle	Tricarboxylic acid cycle
TG	Triglyceride

## Supplementary Information

The online version contains supplementary material available at <https://doi.org/10.1186/s12964-022-01001-3>.

**Additional file 1.** Original data of WB.

**Additional file 2: Figure S1.** Conservative analysis of *LncRNA-TBP* performed by using the NCBI's BLAST. A total of eighteen species, including *Anas platyrhynchos*, *Anser cygnoides*, *Apteryx mantelli mantelli*, *Aquila chrysaetos*, *Bos taurus*, *Coturnix japonica*, *Gallus gallus*, *Geospiza fortis*, *Homo sapiens*, *Meleagris gallopavo*, *Melospittacus undulatus*, *Mus musculus*, *Numida meleagris*, *Ovis aries*, *Pan troglodytes*, *Rattus norvegicus*, *Sus scrofa* and *Zebra finch* were used for Nucleotide BLAST. Top 4 most conservative results were listed above.

**Additional file 3: Figure S2.** Interference of *LncRNA-TBP* promotes myoblast proliferation but inhibits myogenic differentiation. (A-K) Relative *LncRNA-TBP* expression (n = 6) (A), relative mRNA levels of several cell cycle genes (n = 6) (B), EdU proliferation assays (n = 3) (C), proliferation rate of myoblasts (n = 8) (D), CCK-8 assays (n = 6) (E), cell cycle analysis (n = 4) (F), MyHC immunostaining (n = 3) (G), myotube area (n = 8) (H), myoblast fusion index (n = 8) (I), relative mRNA (n = 6) (J) and protein (n = 3) (K) expression levels of myoblast differentiation marker genes with *LncRNA-TBP* interference in vitro. In panel (K), the numbers shown below the bands were folds of band intensities relative to control. Band intensities were quantified by ImageJ and normalized to GAPDH. Data are expressed as a fold-change relative to the control. Results are presented as mean  $\pm$  SEM. In panels (A-B, D-F, and H-J), the statistical significance of differences between means was assessed using an independent sample t-test.

**Additional file 4: Figure S3.** Interference of *LncRNA-TBP* inhibits fatty acid oxidation in skeletal muscle. (A-F) Relative *LncRNA-TBP* expression (n = 4) (A), relative mtDNA content (n = 4) (B), relative fatty acid  $\beta$ -oxidation rate (n = 4) (C), relative FFA and TG content (n = 4) (D), relative mRNA (n = 6) (E) and protein (n = 3) (F) expression levels of fatty acid oxidation or synthesis related-genes in gastrocnemius with *LncRNA-TBP* interference in vivo. In panel (F), the numbers shown below the bands were folds of band intensities relative to control. Band intensities were quantified by ImageJ and normalized to GAPDH. Data are expressed as a fold-change relative to the control. Results are shown as mean  $\pm$  SEM. In panels (A-E), the statistical significance of differences between means was assessed using an independent sample t-test.

**Additional file 5: Figure S4.** Interference of *LncRNA-TBP* activates fast-twitch muscle phenotype and reduces muscle hypertrophy. (A-N) relative enzymes activity of LDH and SDH (n = 4) (A), Relative glycogen content (n = 5) (B), relative mRNA expression levels of glycogenolytic and glycolytic genes (n = 6) (C), relative mRNA expression levels of several fast-/slow-twitch myofiber genes (n = 6) (D), immunohistochemistry analysis of MYH1A/MYH7B (n = 3) (E), MYH1A/MYH7B protein content (n = 8) (F), relative gastrocnemius muscle weight (n = 6) (G), H&E staining (n = 3) (H), relative mRNA (n = 6) (I), and the protein (n = 3) (J) expression levels of the atrophy and autophagy-related genes of in gastrocnemius with *LncRNA-TBP* interference in vivo. In panel (J), the numbers shown below the bands

were folds of band intensities relative to control. Band intensities were quantified by ImageJ and normalized to GAPDH. Data are expressed as a fold-change relative to the control. Results are shown as mean  $\pm$  SEM. In panels (A-D, F and H-I), the statistical significance of differences between means was assessed using an independent sample t-test.

**Additional file 6: Figure S5.** TBP specific target genes identified by ATAC-seq. (A) The RPISeq results showed that the TBP was predicted to interact with *LncRNA-TBP*. (B) Analysis of TBP-targeted binding target genes by ATAC-seq. (C) GO functions analysis of TBP specific binding target genes identified by ATAC-seq. (D) KEGG pathways analysis of TBP specific binding target genes identified by ATAC-seq.

**Additional file 7: Figure S6.** Overexpression and knockdown of *LncRNA-TBP* did not change the mRNA and protein expression level of *TBP*. (A and B) The mRNA level of *TBP* with *LncRNA-TBP* overexpression (n = 6) (A) and knockdown (n = 6) (B) in vitro. (C and D) The protein level of *TBP* with *LncRNA-TBP* overexpression (n = 3) (C) and knockdown (n = 3) (D) in vitro. In panel (C, D), the numbers shown below the bands were folds of band intensities relative to control. Band intensities were quantified by ImageJ and normalized to GAPDH. In panels (A, B), the statistical significance of differences between means was assessed using an independent sample t-test.

**Additional file 8: Figure S7.** Interference of *LncRNA-TBP* inhibit the transcriptional activity of TBP-target genes. (A-G) TBP enrichment at the *KLF4*, *GPI*, *TNNI2*, and *CDKN1A* promoter enrichment (n = 3) (A), relative promoter activity of *KLF4* (B), *GPI* (C), *TNNI2* (D), and *CDKN1A* (E) (n = 4), relative mRNA (n = 4) (F) and protein (n = 3) (G) of *KLF4*, *GPI*, *TNNI2*, and *CDKN1A* with *LncRNA-TBP* interference in vitro. In panel (G), the numbers shown below the bands were folds of band intensities relative to control. Band intensities were quantified by ImageJ and normalized to GAPDH. Data are expressed as a fold-change relative to the control. Results are shown as mean  $\pm$  SEM. In panels (A-F), the statistical significance of differences between means was assessed using an independent sample t-test.

**Additional file 9: Figure S8.** The expression and location analysis of *TBP*. (A) Relative *TBP* expression during the proliferation and differentiation of CPM isolated from XH chicken (n = 4). (B) Subcellular location of *TBP* protein annotated by UniProt Knowledgebase (<https://www.uniprot.org/>). In panels (A), results are presented as mean  $\pm$  SEM.

**Additional file 10.** Supplementary Information.

**Additional file 11: Table S2.** Comparative metabolome analysis of control group versus *LncRNA-TBP* overexpression gastrocnemius.

**Additional file 12: Table S3.** TBP specific target genes identified by ATAC-seq analysis.

## Acknowledgements

Not applicable.

## Author contributions

QN, HX and XZ conceived and designed the study. MM and BC performed the experiments, interpreted the data and wrote the paper. ZZ, SK and JZ performed the experiments. All authors read and approved the final manuscript.

## Funding

This work was supported by National Key R&D Program of China (2021YFD1300100), the Natural Scientific Foundation of China (U1901206 and 31761143014), Local Innovative and Research Teams Project of Guangdong Province (2019BT02N630), China Agriculture Research System (CARS-41-G03), Guangdong Basic and Applied Basic Research Foundation (2021A1515111069), and China Postdoctoral Science Foundation (2022M710052).

## Availability of data and materials

The data that support the findings of this study are available from the corresponding author upon reasonable request.

## Declarations

### Ethics approval and consent to participate

All animal experimental protocols were conformed to “The Instructive Notions with Respect to Caring for Laboratory Animals” issued by the Ministry of Science and Technology of the People’s Republic of China, and approved by the Institutional Animal Care and Use Committee at the South China Agricultural University (approval ID: SCAU#2021c008).

### Consent for publication

Not applicable.

### Competing interests

The authors declare that they have no competing interests.

Received: 25 August 2022 Accepted: 30 October 2022

Published online: 12 January 2023

## References

- Wosczyzna MN, Rando TA. A muscle stem cell support group: coordinated cellular responses in muscle regeneration. *Dev Cell*. 2018;46:135–43.
- Godfrey R, Quinlivan R. Skeletal muscle disorders of glycogenolysis and glycolysis. *Nat Rev Neurol*. 2016;12:393–402.
- Bowen TS, Schuler G, Adams V. Skeletal muscle wasting in cachexia and sarcopenia: molecular pathophysiology and impact of exercise training. *J Cachexia Sarcopenia Muscle*. 2015;6:197–207.
- Buckingham M. Myogenic progenitor cells and skeletal myogenesis in vertebrates. *Curr Opin Genet Dev*. 2006;16:525–32.
- Mishra P, Varuzhanyan G, Pham AH, Chan DC. Mitochondrial dynamics is a distinguishing feature of skeletal muscle fiber types and regulates organellar compartmentalization. *Cell Metab*. 2015;22:1033–44.
- Schiaffino S, Reggiani C. Fiber types in mammalian skeletal muscles. *Physiol Rev*. 2011;91:1447–531.
- Koutakis P, Weiss DJ, Miserlis D, Shostrom VK, Papoutsis E, Ha DM, Carpenter LA, McComb RD, Casale GP, Pipinos II. Oxidative damage in the gastrocnemius of patients with peripheral artery disease is myofiber type selective. *Redox Biol*. 2014;2:921–8.
- Lefaucheur L. Myofiber typing and pig meat production. *Slov Vet Res*. 2001;38:5–28.
- Goodrich JA, Tjian R. TBP-TAF complexes: selectivity factors for eukaryotic transcription. *Curr Opin Cell Biol*. 1994;6:403–9.
- Thomas MC, Chiang CM. The general transcription machinery and general cofactors. *Crit Rev Biochem Mol Biol*. 2006;41:105–78.
- Huang S, Yang S, Guo J, Yan S, Gaertig MA, Li S, Li XJ. Large polyglutamine repeats cause muscle degeneration in SCA17 mice. *Cell Rep*. 2015;13:196–208.
- Yu F, Bracken CP, Pillman KA, Lawrence DM, Goodall GJ, Callen DF, Neilsen PM. p53 represses the oncogenic Sno-MiR-28 derived from a SnoRNA. *PLoS ONE*. 2015;10:e0129190.
- Herrera FJ, Yamaguchi T, Roelink H, Tjian R. Core promoter factor TAF9B regulates neuronal gene expression. *Elife*. 2014;3:e02559.
- Frontini M, Soutoglou E, Argentini M, Bole-Feysot C, Jost B, Scheer E, Tora L. TAF9b (formerly TAF9L) is a bona fide TAF that has unique and overlapping roles with TAF9. *Mol Cell Biol*. 2005;25:4638–49.
- Fieremans N, Van Esch H, Holvoet M, Van Goethem G, Devriendt K, Rosello M, Mayo S, Martinez F, Jhangiani S, Muzny DM, et al. Identification of intellectual disability genes in female patients with a skewed X-inactivation pattern. *Hum Mutat*. 2016;37:804–11.
- Djebali S, Davis CA, Merkel A, Dobin A, Lassmann T, Mortazavi A, Tanzer A, Lagarde J, Lin W, Schlesinger F, et al. Landscape of transcription in human cells. *Nature*. 2012;489:101–8.
- Lu L, Sun K, Chen X, Zhao Y, Wang L, Zhou L, Sun H, Wang H. Genome-wide survey by ChIP-seq reveals YY1 regulation of lincRNAs in skeletal myogenesis. *Embo J*. 2013;32:2575–88.
- Cai B, Li Z, Ma M, Zhang J, Kong S, Abdalla BA, Xu H, Jebessa E, Zhang X, Lawal RA, et al. Long noncoding RNA SMUL suppresses SMURF2 production-mediated muscle atrophy via nonsense-mediated mRNA decay. *Mol Ther Nucleic Acids*. 2021;23:512–26.
- Cai B, Ma M, Chen B, Li Z, Abdalla BA, Nie Q, Zhang X. MIR-16-5p targets SESN1 to regulate the p53 signaling pathway, affecting myoblast proliferation and apoptosis, and is involved in myoblast differentiation. *Cell Death Dis*. 2018;9:367.
- Ma M, Cai B, Jiang L, Abdalla BA, Li Z, Nie Q, Zhang X. lncRNA-Six1 Is a Target of miR-1611 that functions as a ceRNA to regulate Six1 protein expression and fiber type switching in chicken myogenesis. *Cells*. 2018;7:243.
- Ding L, Yang X, Tian H, Liang J, Zhang F, Wang G, Wang Y, Ding M, Shui G, Huang X. Seipin regulates lipid homeostasis by ensuring calcium-dependent mitochondrial metabolism. *Embo J*. 2018;37:e97572.
- Wallace DC. Mitochondria and cancer. *Nat Rev Cancer*. 2012;12:685–98.
- Wang T, Xu YQ, Yuan YX, Xu PW, Zhang C, Li F, Wang LN, Yin C, Zhang L, Cai XC, et al. Succinate induces skeletal muscle fiber remodeling via SUNC1 signaling. *EMBO Rep*. 2019;20:e47892.
- Yang X, Brobst D, Chan WS, Tse M, Herlea-Pana O, Ahuja P, Bi X, Zaw AM, Kwong Z, Jia WH, et al. Muscle-generated BDNF is a sexually dimorphic myokine that controls metabolic flexibility. *Sci Signal*. 2019;12:eaau1468.
- Braun T, Gautel M. Transcriptional mechanisms regulating skeletal muscle differentiation, growth and homeostasis. *Nat Rev Mol Cell Biol*. 2011;12:349–61.
- Mizushima N, Levine B, Cuervo AM, Klionsky DJ. Autophagy fights disease through cellular self-digestion. *Nature*. 2008;451:1069–75.
- Joseph AM, Adhithetty PJ, Leeuwenburgh C. Beneficial effects of exercise on age-related mitochondrial dysfunction and oxidative stress in skeletal muscle. *J Physiol*. 2016;594:5105–23.
- Huarte M, Guttman M, Feldser D, Garber M, Koziol MJ, Kenzelmann-Broz D, Khalil AM, Zuk O, Amit I, Rabani M, et al. A large intergenic noncoding RNA induced by p53 mediates global gene repression in the p53 response. *Cell*. 2010;142:409–19.
- Dynlacht BD, Hoey T, Tjian R. Isolation of coactivators associated with the TATA-binding protein that mediate transcriptional activation. *Cell*. 1991;66:563–76.
- Heller H, Bengal E. TFIID (TBP) stabilizes the binding of MyoD to its DNA site at the promoter and MyoD facilitates the association of TFIIB with the preinitiation complex. *Nucleic Acids Res*. 1998;26:2112–9.
- Jallow Z, Jacobi UG, Weeks DL, Dawid IB, Veenstra GJ. Specialized and redundant roles of TBP and a vertebrate-specific TBP paralog in embryonic gene regulation in *Xenopus*. *Proc Natl Acad Sci U S A*. 2004;101:13525–30.
- Ravarani C, Flock T, Chavali S, Anandapadamanaban M, Babu MM, Balaji S. Molecular determinants underlying functional innovations of TBP and their impact on transcription initiation. *Nat Commun*. 2020;11:2384.
- Buckingham M, Rigby PW. Gene regulatory networks and transcriptional mechanisms that control myogenesis. *Dev Cell*. 2014;28:225–38.
- Wang S, Zuo H, Jin J, Lv W, Xu Z, Fan Y, Zhang J, Zuo B. Long noncoding RNA Neat1 modulates myogenesis by recruiting Ezh2. *Cell Death Dis*. 2019;10:505.
- Li Y, Chen X, Sun H, Wang H. Long non-coding RNAs in the regulation of skeletal myogenesis and muscle diseases. *Cancer Lett*. 2018;417:58–64.
- Ismail I, Joo ST. Poultry meat quality in relation to muscle growth and muscle fiber characteristics. *Korean J Food Sci Anim Resour*. 2017;37:873–83.
- Ryu YC, Kim BC. The relationship between muscle fiber characteristics, postmortem metabolic rate, and meat quality of pig longissimus dorsi muscle. *Meat Sci*. 2005;71:351–7.
- Park BY, Kim NK, Lee CS, Hwang IH. Effect of fiber type on postmortem proteolysis in longissimus muscle of Landrace and Korean native black pigs. *Meat Sci*. 2007;77:482–91.
- Hu H, Wang J, Zhu R, Guo J, Wu Y. Effect of myosin heavy chain composition of muscles on meat quality in Laiwu pigs and Duroc. *Sci China C Life Sci*. 2008;51:127–32.
- Zurlo F, Larson K, Bogardus C, Ravussin E. Skeletal muscle metabolism is a major determinant of resting energy expenditure. *J Clin Invest*. 1990;86:1423–7.
- Berkes CA, Tapscott SJ. MyoD and the transcriptional control of myogenesis. *Semin Cell Dev Biol*. 2005;16:585–95.

42. Zhao DM, Zhu SQ, Wang FR, Huang SS. Role of mutant TBP in regulation of myogenesis on muscle satellite cells. *Curr Med Sci.* 2019;39:734–40.
43. Li N, Richard S. Sam68 functions as a transcriptional coactivator of the p53 tumor suppressor. *Nucleic Acids Res.* 2016;44:8726–41.
44. Jin JJ, Lv W, Xia P, Xu ZY, Zheng AD, Wang XJ, Wang SS, Zeng R, Luo HM, Li GL, et al. Long noncoding RNA SYSL regulates myogenesis by interacting with polycomb repressive complex 2. *Proc Natl Acad Sci U S A.* 2018;115:E9802–11.
45. Sui Y, Han Y, Zhao X, Li D, Li G. Long non-coding RNA lrm enhances myogenic differentiation by interacting with MEF2D. *Cell Death Dis.* 2019;10:181.

### Publisher's Note

Springer Nature remains neutral with regard to jurisdictional claims in published maps and institutional affiliations.

Ready to submit your research? Choose BMC and benefit from:

- fast, convenient online submission
- thorough peer review by experienced researchers in your field
- rapid publication on acceptance
- support for research data, including large and complex data types
- gold Open Access which fosters wider collaboration and increased citations
- maximum visibility for your research: over 100M website views per year

At BMC, research is always in progress.

Learn more [biomedcentral.com/submissions](https://biomedcentral.com/submissions)

